SIT-P102 (9/63)

UNPUBLISHED PRELIMINARY DATA

UNCLASSIFIED

FINAL REPORT

September 1963

by

Jack Fajans

and

Carol Rosen

Sep. 1963

DEPARTMENT OF PHYSICS

t! Theoretical and Experimental Aspects of the Electrohydrodynamics of Superfluid Helium

and

Focussing of Phonons in Superfluid Helium below 0.5° Kelvin , Final Report

8360000

Contract No. (NASA Grant NsG-130-61)

Office of Research Grants and Contracts

Code SC, National Aeronautics and Space Admin.

1520 H Street, N. W.

Washington 25, D. C.

STEVENS INSTITUTE OF TECHNOLOGY

CASTLE POINT STATION
HOBOKEN, NEW JERSEY

Repts. (NASACR-55303) SIT-P102 (9/63)

OTS:

UNCLASSIFIED

FINAL REPORT

September 1963

by

Jack Fajans

and

Carol Rosen Sep. 1963 34 p n/a

DEPARTMENT OF PHYSICS

STEVENS INSTITUTE OF TECHNOLOGY

CASTLE POINT STATION

HOBOKEN, NEW JERSEY
N.J.

$360 000

Theoretical and Experimental Aspects of the Electrohydrodynamics of Superfluid Helium and Focussing of Phonons in Superfluid Helium below 0.5° Kelvin

Final ...

Contract No. NASA Grant NsG-130-61

Office of Research Grants and Contracts

Code SC, National Aeronautics and Space Admin.

1520 H Street, N. W.

Washington 25, D. C.

FINAL REPORT

NASA Grant #NsG-130-61

Experimental and theoretical studies on the electrohydrodynamics of superfluid helium were the principal concern of the grant supported research.

Three technical papers listed immediately following have described in detail completed portions of the work.

1. W. J. Neidhardt and J. Fajans, "Electrodynamics of Superfluid Helium in Narrow Channels", Phys. Rev. 128, 495 (1962). (attached)

2. J. K. Percus, "Macroscopic Modes of He II, Proceedings of VIII Int'l. Low Temp. Conf. (1962). (attached)

3. F. Pollock, "The Use of Electric Fields in the Investigation of the Structure of Liquid and Solid Helium", submitted as a research proposal to NASA in September 1961. (attached)

Paper (2) is pertinent to an understanding of the velocity dependence of superfluid helium at pressure differences such that fluid flow is below the critical velocity i.e., in the absence of viscosity.

Paper (3) is a research proposal written by the Physics Faculty at Stevens. It presents a theoretical study of various ways in which electric fields affect the structure of liquid helium. In particular the dielectric constant of superfluid helium is examined as a function of pressure and electric field, and an estimate is made of the effect of electric field on the λ transition. It describes the motivation for studies of the superfluid under the action of externally applied electric fields.

The unpublished work (previously reported in the semi-annual reports) is summarized below.

I. Construction of a new cryostat and associated equipment for measurements of critical velocities and the effect of electric fields on critical flow was initiated and brought to ninety per cent completion. Specific elements of the apparatus which were completed are:

A. Appropriate vacuum jackets, pumping systems and physical supports. The extremely sensitive manometer system necessitated isolation of the cryostat from vibration and precise leveling.

B. A variable width flow channel in which support of macroscopic fields of six to ten million volts/cm was anticipated. Two major improvements over the channel reported on in reference (1) were: a) Provision of the ability to measure pressure directly and accurately at both ends of the channel; b) Doubling of the supported electric field strength.

C. Remotely operable liquid helium fill valves which could provide effective seal to flow of superfluid.

D. A liquid helium level alpha-particle gage sensitive to less than one ten thousandth of a centimeter of helium. Coupled with a manometer, pressure differentials smaller than one millionth of a cm Hg might be detected with a measurement time constant of one second.

E. Bridge circuits for measuring alpha-particle ionization currents.

This construction represents a very substantial portion of the entire amount of effort required in carrying through such an experiment to completion.

II. Construction was completed and experiments initiated on an apparatus for focussing phonons in superfluid helium. The major support in this area was to a doctoral student for making operative an apparatus

eighty per cent completed.

A simulated run was performed using He^4 as the refrigerant instead of He^3. The minimum temperature of the He^4 bath was 1.25°k. This was encouraging since the temperature estimated for this experiment was 1.30°k. The temperature of the experimental chamber was 0.99°k obtained from a He^4 vapor pressure reading of 108 μ. This pressure, if due to the He^3, would produce a temperature of 0.47°k. But the compressibilities of He^4 and He^3 are not the same in this temperature range, and the heat leaks encountered are sufficiently different for the isotopes, so that an exact calculation from these results of the expected He^3 temperature is impractical.

However, since the estimated He^3 temperature for the experiment is between 0.45°k and 0.5°k these results have led to the preparations, which are now being completed, for an actual run using He^3 as the refrigerant.

The helium 4 pumping system for both experiments I and II is illustrated in Figure 1. In practice an experimental chamber is immersed in the helium bath and supported by appropriate vacuum-tight tubing coming out through the top of this dewar.

Figure 2 is a photograph of parts A, B, and C of experiment I.

Figures 3, 4, and 5 are photographs of experiment II. The one inch formica disk in Figure 4 supports two opposite 90° arcs of carbon each 0.015 inches thick and 1.4×10^{-3} square inches in area. The carbon electrodes act as the phonon source and the phonon receiver. This disk

with its carbon-face down, screws onto the brass cup on the right which houses the fused quartz concave focussing mirror. The mirror moves through a 5 degree arc by means of the electromagnet shown in Figure 3. The brass cup fits inside the cylindrically shaped copper experimental chamber, to its right. The wires shown hanging from the base of the He^3 circulatory system are connected by silver epoxy to brass rivets on the non-carbon side of the formica disk. Ground connections are made to each carbon electrode. The copper chamber is soldered to the copper base of the stainless steel He^3 system, and the brass vacuum jacket on the extreme right of the photograph encloses the experimental chamber. Figure 5 is a closeup of the base of the He^3 refrigerating system. The winding monel capillary (I.D. = 10 mils) throttles the compressed He^3 into the half-inch stainless steel tube. Each of the two binding posts connect a 1 mil teflon coated wire, which comes down through six feet of monel capillary (I.D. = 10 mils), to one of the two carbon electrodes. These two monel capillaries also carry the helium 4 into the experimental chamber. The ends of these monel capillaries are seen between the binding posts in Figure 5 and to the left of the binding posts in Figure 4.

Technical personnel engaged in grant activity and supported by grant funds were Professors J. Fajans, J. K. Percus, and F. Pollock and graduate students W. J. Neidhardt and C. Rosen. Neidhardt received a Ph.D degree in 1962. Rosen continues research on a doctoral dissertation at the time of writing of this final report.

A liquid helium flow regulator which has no moving parts was invented during the course of the work. The principle is substantially described in the paper (1).

SUMMARY

Grant funds supported

a. Research for the three papers cited above.

b. Construction of apparatus for two new liquid helium researches different from the research described in a.

c. Invention of a new type of liquid helium flow regulator.

d. Two graduate students one of whom received a Ph.D degree.

APPENDIX

Copies of papers cited

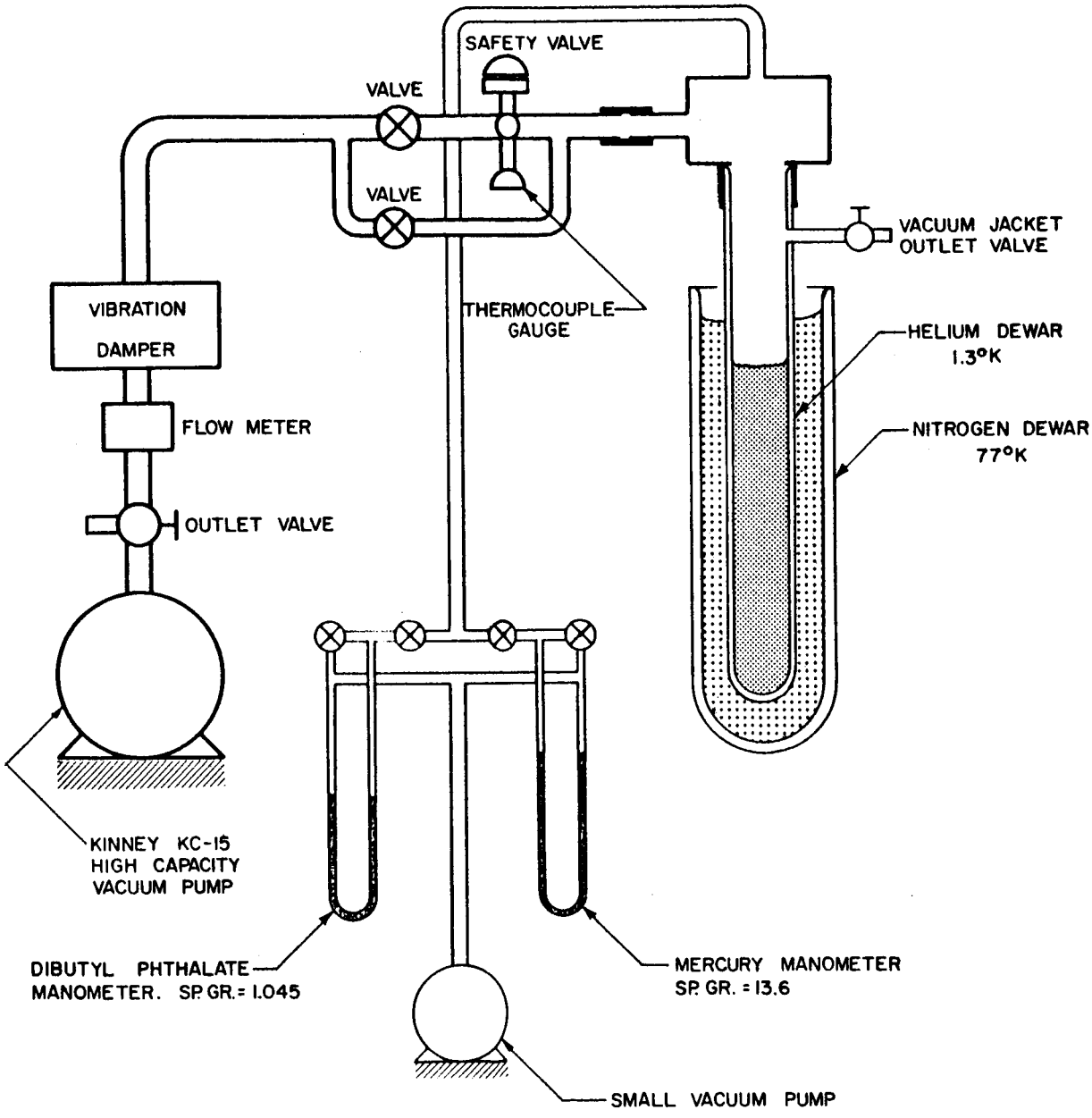

FIGURE 1 BLOCK DIAGRAM OF HELIUM PUMPING SYSTEM

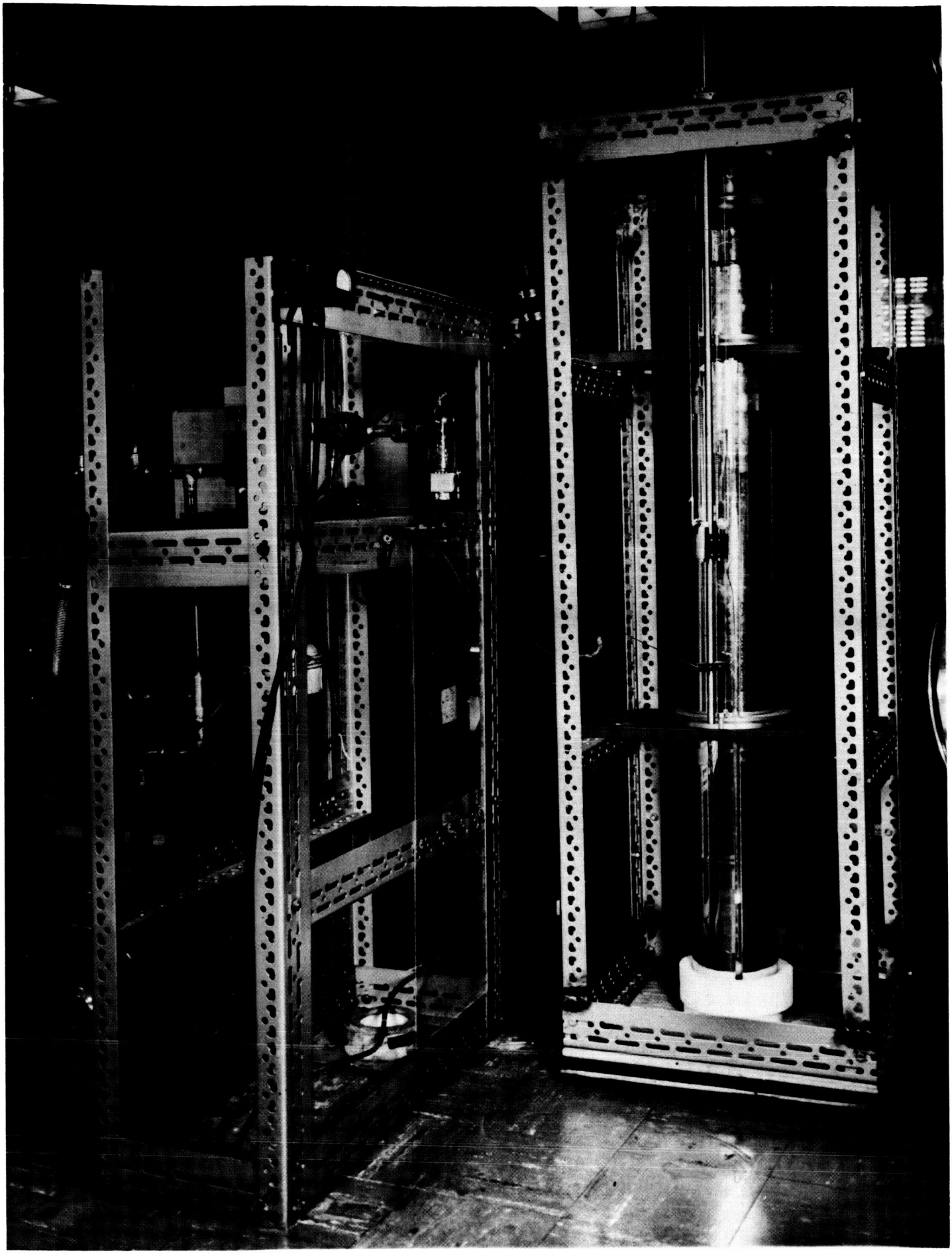

FIG. 2

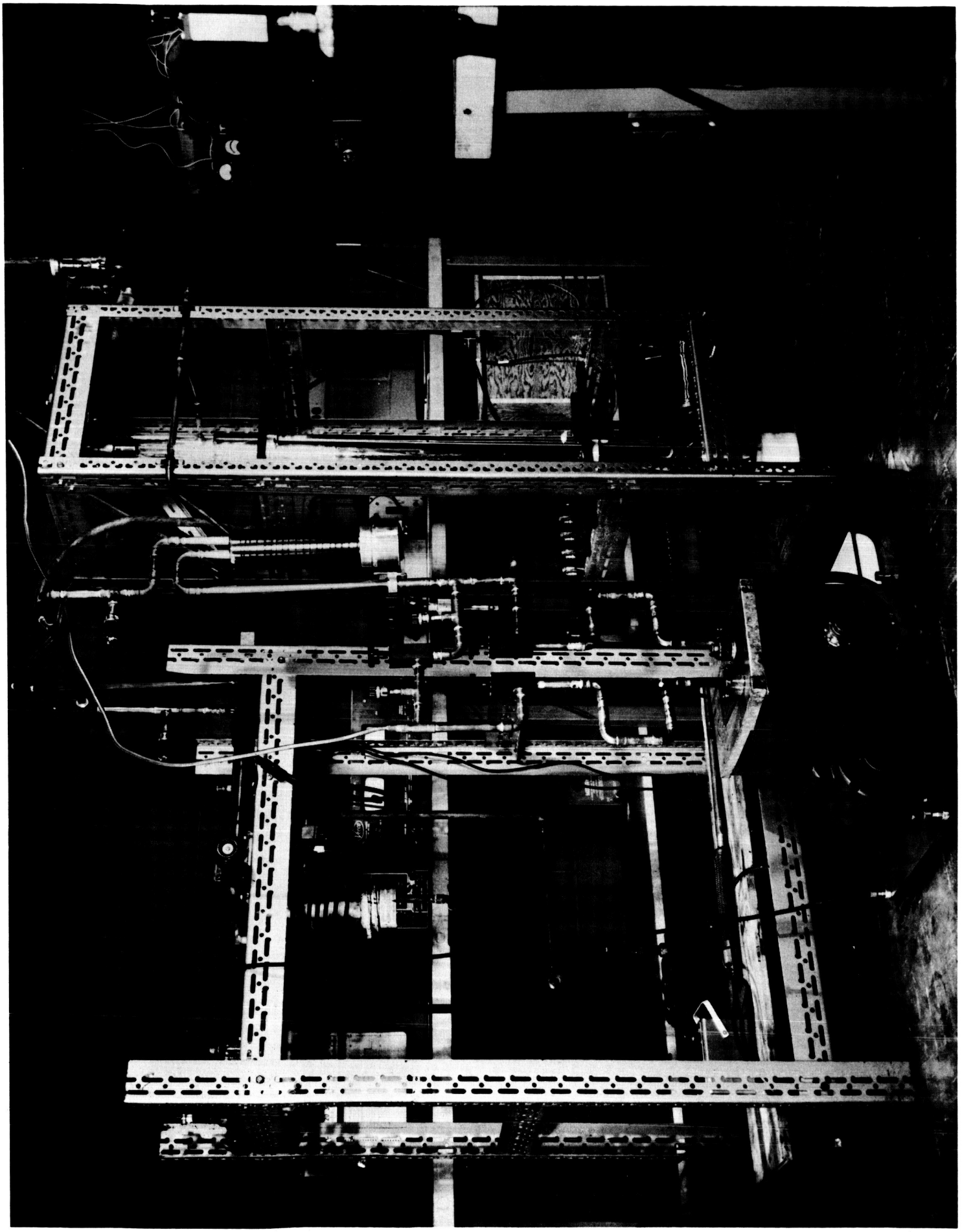

FIG. 3

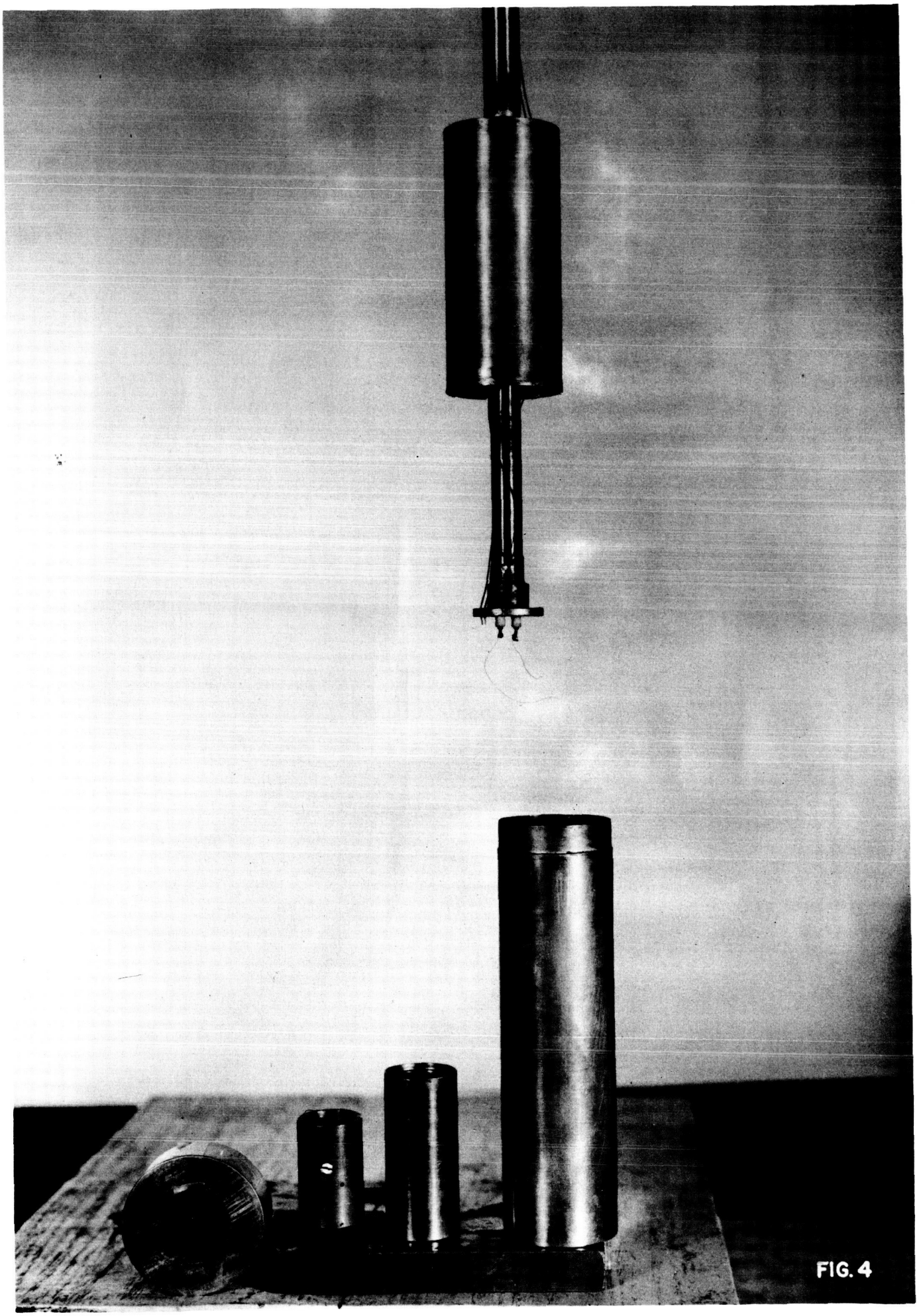

FIG. 4

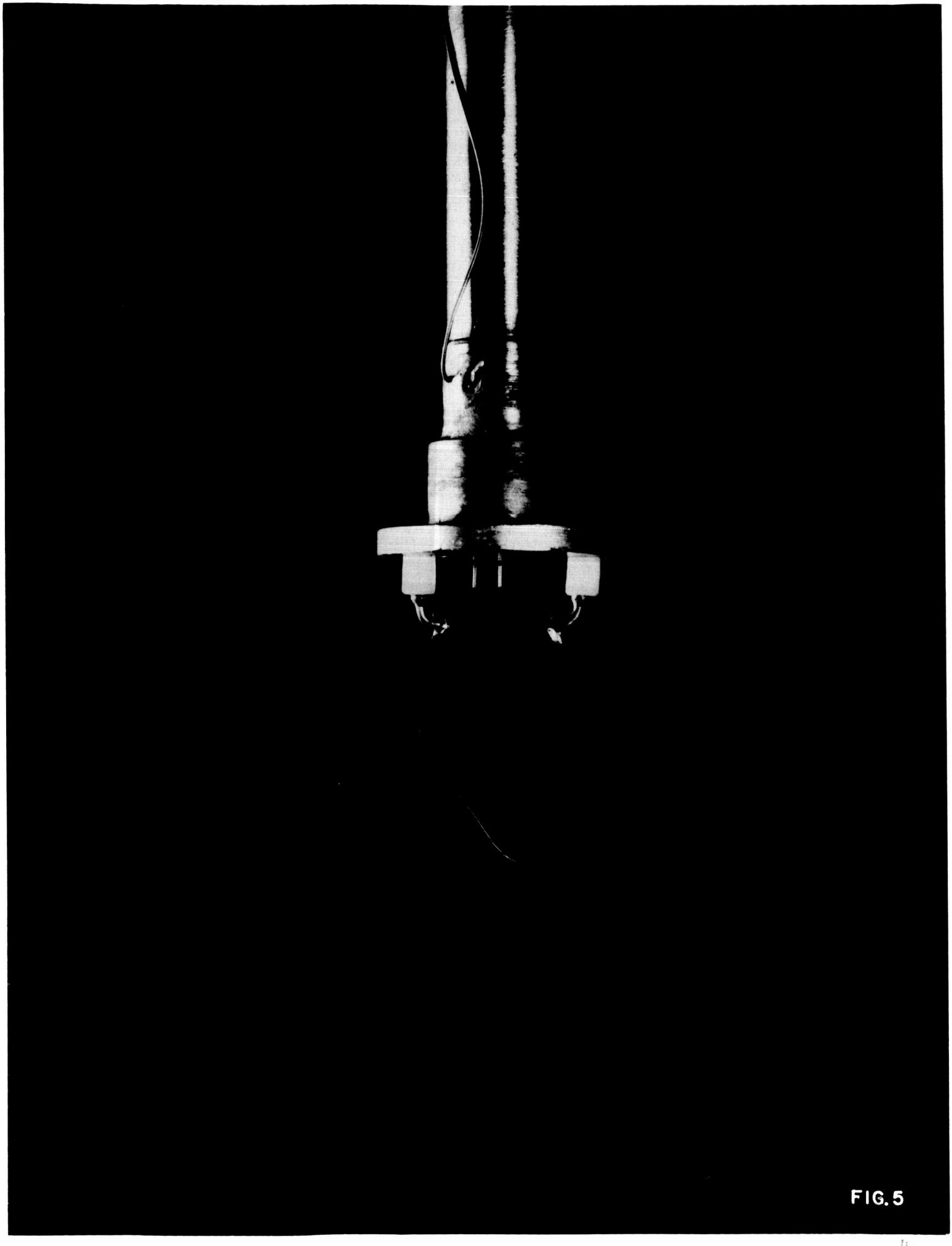

FIG. 5

Reprinted from THE PHYSICAL REVIEW, Vol. 128, No. 2, 495–502, October 15, 1962
Printed in U. S. A.

Electrohydrodynamics of Superfluid Helium in Narrow Channels*

W. JIM NEIDHARDT† AND JACK FAJANS
Stevens Institute of Technology, Hoboken, New Jersey

(Received June 8, 1962)

The flow of superfluid helium from a liquid reservoir to vacuum through a 10^{-5} cm channel, which was enhanced tenfold by an electric field of 3×10^6 V/cm when a phase boundary occurred within the channel, was unaffected when the boundary moved past the channel and field. Superfluid flow at subcritical velocity given by $\Gamma-\Gamma_0=f(T)V^2$, when increased to critical flow under the influence of electrostrictive pressures was given by $\Gamma=[\rho_n/\rho][\eta(T_\lambda)/\eta(T)]K_n+[\rho_s/\rho]K_s$, with Γ and Γ_0 the flow with and without applied electric field, V the applied voltage, T the temperature, ρ_n and ρ_s the normal and superfluid densities, ρ the total density, η the viscosity, and K_n and K_s flows obtained from normalization of data. A coincidence was noted between a maximum at 2.08°K in the relative flow and an already reported maximum at 2.10°K in thermal boundary conduction. Any shift in the λ point induced by a macroscopic field of 1.5×10^6 V/cm was less than 0.02°K, but displacements as great as 0.5°K were induced by use of very fine channels.

INTRODUCTION

HELIUM transport under the influence of electric fields may appropriately be termed electrohydrodynamic in the instant investigation, since electrostrictive forces and forces derived from dielectric gradients substantially altered the field free flow pattern. The origin of the net electrostrictive forces and dielectric gradients was a liquid-vapor interface in the strong-field region of the narrow channels which were used.

A number of earlier related papers may be cited. The work of Giauque *et al.*[1] had characteristics similar to those of our field-free flow, and extensive work has been carried out on field-free flow with liquid-helium reservoirs at both ends of the channel (i.e., without an interior phase boundary).[2–4]

Dielectric breakdown at fields of 10^6 V/cm was established by Blank and Edwards[5] for stationary liquid helium between spherical electrodes 0.15 mm apart; nevertheless, in the present experiment fields of 3×10^6 V/cm were employed.

McCrum and Eisenstein[6] have suggested that boundary fields alter the superfluid behavior of liquid helium in films and fine channels. The lowering of the λ-transition temperature in the flow of unsaturated superfluid film[7] and of liquid in fine channels[8] may be caused by intense electric fields at the liquid substratum boundary.

EXPERIMENT

The amount of helium flowing from a liquid reservoir through a superleak, Fig. 1, to an evacuated chamber at room temperature was obtained by measuring the collected gas. The flow channel was the space between the stainless steel and fluorlin arising from submicroscopic imperfections in the surfaces which persisted after compression of the assembly by a spring. A poten-

* This work was made possible through support provided by the Office of Scientific Research, U. S. Air Force, and the National Aeronautics and Space Administration.

† Present address: Newark College of Engineering, Newark, New Jersey.

[1] W. F. Giauque, J. W. Stout, and E. R. Barieau, J. Am. Chem. Soc. 61, 654 (1939).

[2] J. F. Allen and A. D. Misener, Proc. Roy. Soc. (London) A172, 467 (1939).

[3] R. Bowers and K. Mendelssohn, Proc. Phys. Soc. (London) A63, 178 (1950); Proc. Roy. Soc. (London) A213, 158 (1952).

[4] K. R. Atkins, Phil. Mag. Suppl. 1, 169 (1952).

[5] C. Blank and M. H. Edwards, Phys. Rev. 119, 50 (1960).

[6] N. G. McCrum and J. C. Eisenstein, Phys. Rev. 99, 1326 (1955).

[7] E. Long and L. Meyer, Phys. Rev. 79, 1031 (1950); 85, 1030 (1952).

[8] K. R. Atkins, H. Seki, and E. V. Condon, Phys. Rev. 102, 582 (1956).

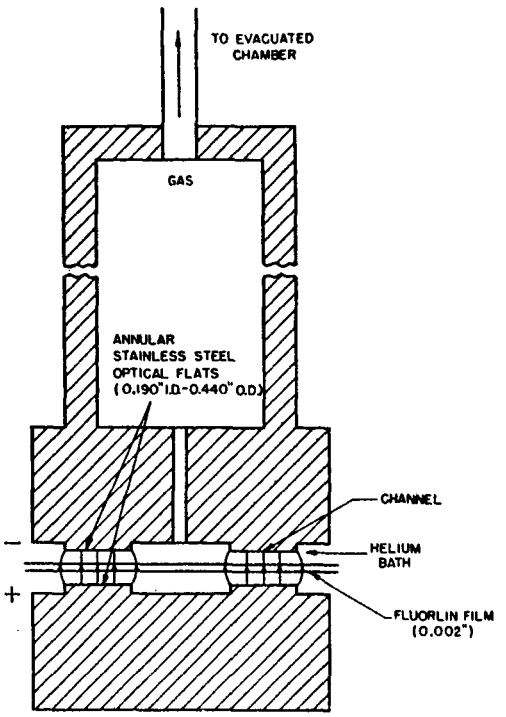

FIG. 1. Representation of components of flow channel before compression by a spring (not shown) to 600-950 psi. Electric field was confined substantially to the region designated. Flow occurred through a channel 10^{-5} cm thick between the fluorlin film and the stainless-steel surface.

tial difference of 0-8000 V dc applied across the fluorlin film between the annular optical flats produced fields up to 3×10^6 V/cm in the helium channel. The electrostatic attraction between the flats, which was usually less than 3% of the spring force and always less than 10% of it, affected the channel size slightly.

The flow rate Γ in atoms per second was computed from

$$\Gamma=(v/kT)(\Delta P/\Delta t), \tag{1}$$

where v, T, and $\Delta P/\Delta t$ were the volume, temperature, and rate of pressure rise of the collection chamber, and k is Boltzmann's constant. A macroscopic electric field E was computed from

$$E\approx(V/d)(\kappa_F/\kappa_H), \tag{2}$$

under the assumption that the fluorlin film thickness, $d=5\times10^{-3}$ cm, was much greater than the helium channel thickness, 10^{-5} cm. V was the applied voltage, $\kappa_F=2.0$ the dielectric constant of fluorlin, and $\kappa_H=1.05$ the dielectric constant of liquid helium. The macroscopic field E was indicative of the microscopic fields in the channel.

Electrostriction

Following Stratton's[9] presentation, the force per unit volume exerted by an electric field on a dielectric fluid is

$$\mathbf{f}=-\tfrac{1}{2}\epsilon_0E^2\nabla\kappa+\tfrac{1}{2}\epsilon_0\nabla(E^2\tau d\kappa/d\tau), \tag{3}$$

where τ is the mass density. The first term is significant for an inhomogeneous dielectric; the second is referred to as the electrostriction term. Using the Clausius-Mossotti relationship

$$(\kappa-1)/(\kappa+2)=c\tau \tag{4}$$

to give the dependence of κ on τ, (3) becomes

$$\mathbf{f}=-\tfrac{1}{2}\epsilon_0E^2\nabla\kappa+\tfrac{1}{6}\epsilon_0\nabla[E^2(\kappa-1)(\kappa+2)]. \tag{5}$$

In equilibrium the electric body forces (5) acting on a fluid are related to the pressure gradient ∇P by

$$\nabla P=-\tfrac{1}{2}\epsilon_0E^2\nabla\kappa+\tfrac{1}{6}\epsilon_0\nabla[E^2(\kappa-1)(\kappa+2)]. \tag{6}$$

Figure 2(a) depicts helium flowing from a reservoir of liquid 1 through a channel of length l and thickness t to a region of vacuum 4. A liquid-gas interface demarcates the liquid 2 in the channel from the channel gas 3, and an electric field is applied along the entire channel length.

Integration of Eq. (6) leads to the equilibrium pressure distribution shown in Figs. 2(b) and 2(c). In Fig. 2(b) the effect of the electrostriction term is broken nto three parts: $\Delta P_{12}^{(\epsilon)}$ the change at the channel entrance, $\Delta P_{23}^{(\epsilon)}$ the change at the interface, and $\Delta P_{34}^{(\epsilon)}$ the change at the exit. The effect of the $\nabla\kappa$ term at the interface is designated $\Delta P_{23}^{(\kappa)}$. $P_v+\Delta h$ gives the sum of vapor pressure and gravitational (hydrostatic) pressure, and $\Delta P'\approx\Delta P_{12}^{(\epsilon)}$.

In Fig. 2(c) the total pressure is plotted, and the slight dip shown at the interface is computed on the basis of constant field strength. In the actual experiment, the electric field in the gas channel was slightly greater than the field in the liquid channel with, correspondingly, a small increase in pressure at the interface. Figures 2(b)–(g) represent only the fluid pressure distribution and do not display electric or thermomechanical body forces.

For an applied potential difference of 4000 V which gave rise to a macroscopic field $E=1.5\times10^6$ V/cm, $\Delta P_{12}^{(\epsilon)}$ was 36 mm Hg. The quantities $\Delta P_{23}^{(\epsilon)}$ and $\Delta P_{23}^{(\kappa)}$ were also approximately this size; the pressure dip at the interface in Fig. 2(c) is exaggerated.

Procedure

The pressure in the collection chamber, measured with an Alphatron gauge was plotted as a function of time for a given temperature and value of electric field, and the flow rate was determined from the slope in the linear region of this plot with Eq. (1). When the time interval of collection was sufficiently long, the pressure in the collection chamber reached a limiting value equal to the vapor pressure of the bath liquid for all electric fields and channel sizes.

[9] J. A. Stratton, *Electromagnetic Theory* (McGraw-Hill Book Company, Inc., New York, 1941), pp. 137–151.

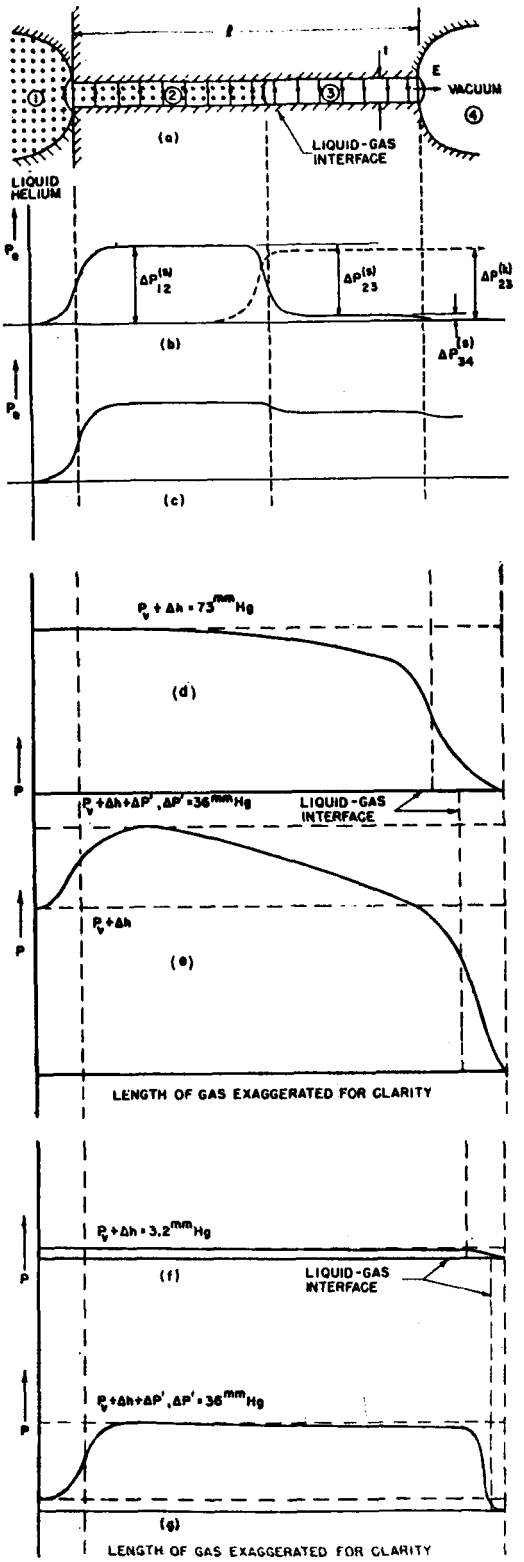

FIG. 2. Pressure distributions in channel with liquid-gas interface and macroscopic electric field. (a) Portrayal of channel; (b) components of *equilibrium* pressure induced by field; (c) total *equilibrium* pressure induced by field; (d) field-free pressure distribution in *flowing* normal fluid; (e) distribution in *flowing* normal fluid with 1.5×10^{6} V/cm; (f) field-free distribution in *flowing* superfluid; (g) distribution in *flowing* superfluid with 1.5×10^{6} V/cm.

A typical flow measurement below the λ point required 13 min. During this interval the pressure in the collection chamber rose to 800 μ Hg and the bath temperature was controlled to 0.002°K. Flow measurements at a given temperature and field were always repeated, and most measurements were taken in order of either ascending or descending temperature.

RESULTS

The channel thickness t for size A (discussed below) channels was estimated from measurements of air flow at $T=293$°K. The linear rise of flow with pressure differential observed experimentally was indicative of Knudsen flow, and t was found to be 3×10^{-5} cm on the basis of flow between parallel planes.

From the data in the temperature range 4.2°K to the λ point another estimate of the channel thickness was made. The pressure distributions of Figs. 2(d) and 2(e) follow from the assumption of laminar liquid flow from the channel entrance to the interface and "slip" flow[10] in the gas from the interface to the exit. The pressures at the interface were calculated for the temperature range from the various measured quantities—flow, entrance pressure, etc.—with an assumed value of channel thickness.

The most plausible set of interface pressures rather sharply defined 1.2×10^{-5} cm as the thickness of a size A channel. The pressure at the interface was lower than the bath vapor pressure because of the evaporative cooling at the interface as well as the dynamic or nonequilibrium flow condition. To the viscous loss in the field-free liquid flow was added essentially all of the electrostrictive pressure $\Delta P_{12}^{(e)}$ when the voltage was applied. The discrepancy between the two determinations of thickness was most likely due to the inadequacy of representing the channel as a pair of parallel planes.

Superfluid Flow

Classification of channel size by the magnitude of the flow rate as in Fig. 3 led to a rough correlation of flow characteristics with and without applied electric field. From the size of the largest class A (maximum $\Gamma_0\approx2\times10^{18}$) to the size of the smallest class D (maximum $\Gamma_0\approx0.3\times10^{18}$), the pressure exerted on the fluorlin film by the annular optical flats varied from 600 to 950 psi (Γ_0 was the field free flow).

The maximum in Γ, exemplified in Fig. 3, was most pronounced for channels with the largest flow rates. As the channel decreased in size the maximum appeared at lower temperatures; for the smallest channel size the maximum was not reached even at 1.30°K, the lowest temperature attained.

[10] R. D. Present, *Kinetic Theory of Gases* (McGraw-Hill Book Company, Inc., New York, 1958), p. 63.

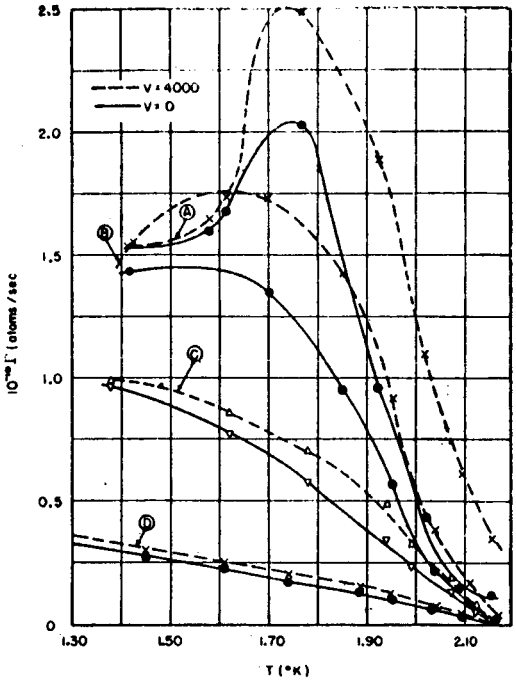

FIG. 3. Superfluid flow in channels of various sizes with and without field.

Figure 4 shows a maximum in the relative increase in flow rate $(\Gamma-\Gamma_0)/\Gamma_0$ for V=4000 V near 2.08°K. The maximum appeared at this temperature for all applied voltages, Fig. 5, and was quite pronounced in the larger channel sizes. However, for channel size *D* it was not observed at any temperature. Perhaps by no more than a coincidence, a maximum in thermal conduction from a wall to superfluid has been noted at 2.1°K by White

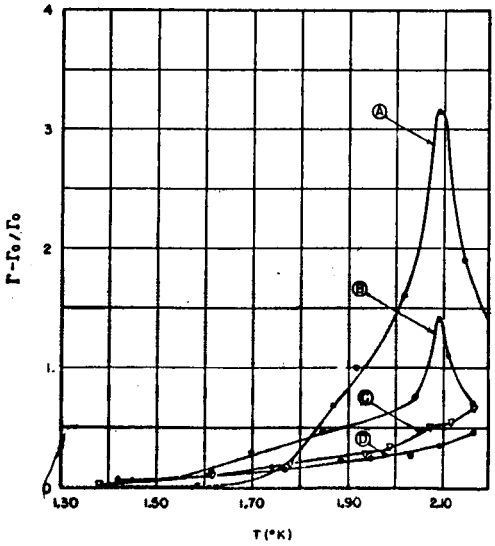

FIG. 4. Relative flow augmentation in channels of various sizes for field of 1.5×10^{-6} V/cm.

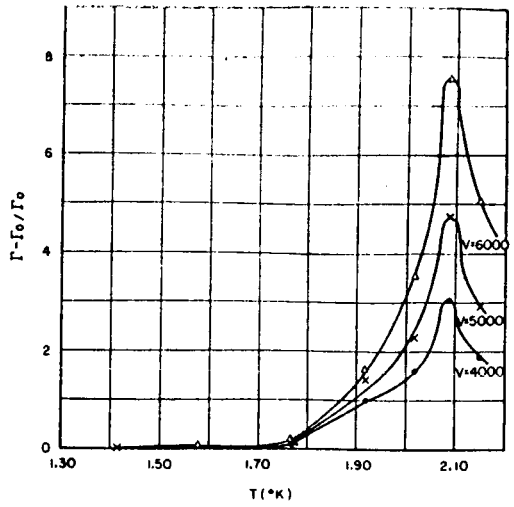

FIG. 5. Relative flow augmentation in a size *A* channel for various fields.

et al.[11] and by Andronikashvili and Mirskaia.[12] The flow was tenfold enhanced in some size *A* channels by a field of 3×10^6 V/cm.

Critical Velocity

The saturation values of Γ evident in the plots vs temperature and voltage presented in Figs. 6–8 are attributed to the superfluid's attainment of critical velocity[13] at high fields. At low fields the superfluid velocity was subcritical. That the liquid-gas interface eventually reached the channel exit is attested to by the maxima of Fig. 6 and by the ineffectiveness of the field in the low-temperature region. The crossed curves of Fig. 8 also manifest this.

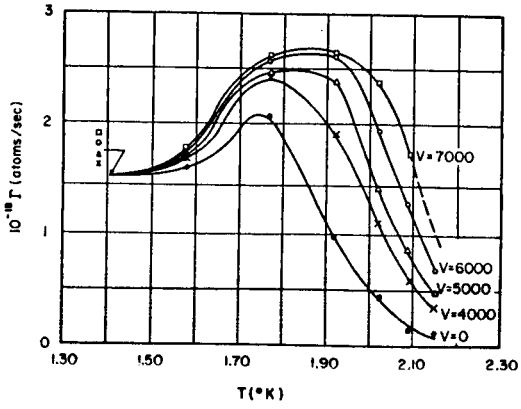

FIG. 6. Flow in an *A* channel for various fields.

[11] D. White, O. D. Gonzales, and H. L. Johnson, Phys. Rev. 89, 593 (1953).
[12] E. L. Andronikashvili and G. G. Mirskaia, J. Exptl. Theoret. Phys. (U.S.S.R.) 29, 490 (1955).
[13] K. R. Atkins, *Liquid Helium* (Cambridge University Press, New York, 1959), pp. 88–91, 198–201.

Giauque, Stout, and Barieau[1] observed similar results for experiments where the entrance of a channel of width 10^{-4} cm was in liquid helium and the exit connected to an evacuated chamber. Their results, also, can be explained by assuming that at the lowest temperatures the liquid-gas interface moved past the exit of the channel thereby causing the flow rate to drop.

In the region of subcritical velocity $\Gamma-\Gamma_0$ was found to be proportional to V^n, where $n=2.0\pm0.5$ (with extreme variation in n given). Figure 9 shows a log plot for a run representative of channel size A. No correlation between n and channel size was found. Each size, possessed high and low values of n, although n was constant during the run of any particular day.

Below the λ point the large rise in flow at zero field with decreasing temperature was due to the superfluid contribution to liquid flow. If it had been flowing at

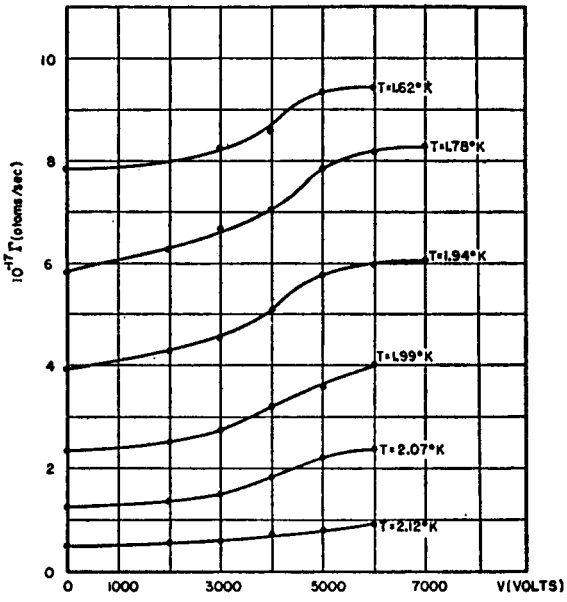

FIG. 7. Flow in a C channel for various temperatures.

critical velocity which is almost independent of temperature, the resulting flow rate would have been given by

$$\Gamma=(\rho_s/\rho)(L/M)\rho A u_c, \tag{7}$$

where A is the cross-sectional area of the channel, L is Avogadro's number, M is the gram atomic weight of helium, u_c is the critical velocity, ρ_s is the superfluid density, and ρ is the density.

Actually, Γ increased more slowly than ρ_s/ρ with decreasing temperature, indicating that the superfluid was flowing below critical velocity. This smaller flow may be attributed to the retarding thermomechanical[14] pressure, which arose from the temperature differential created by the evaporation of liquid inside the channel.

[14] Fritz London, *Superfluids* (John Wiley & Sons, Inc., New York, 1954), Vol. II, p. 70.

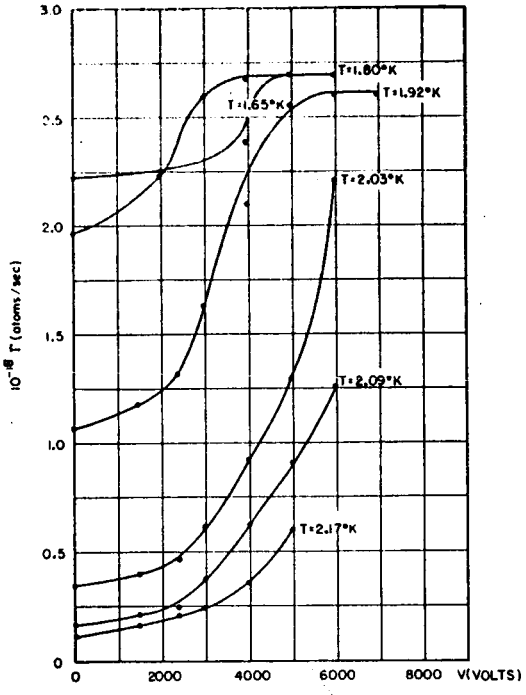

FIG. 8. Flow in an A channel for various temperatures.

The magnitude of this pressure was

$$\Delta P=\rho S\Delta T, \tag{8}$$

where S is the entropy per gram, ΔP was the pressure

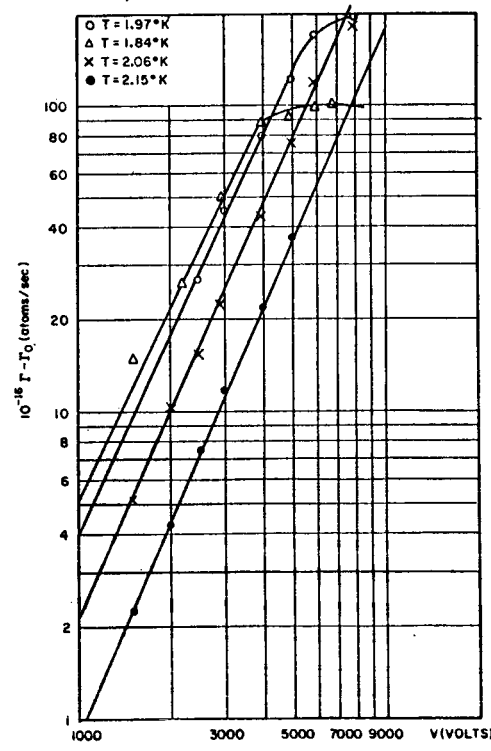

FIG. 9. Flow in an A channel for various temperatures.

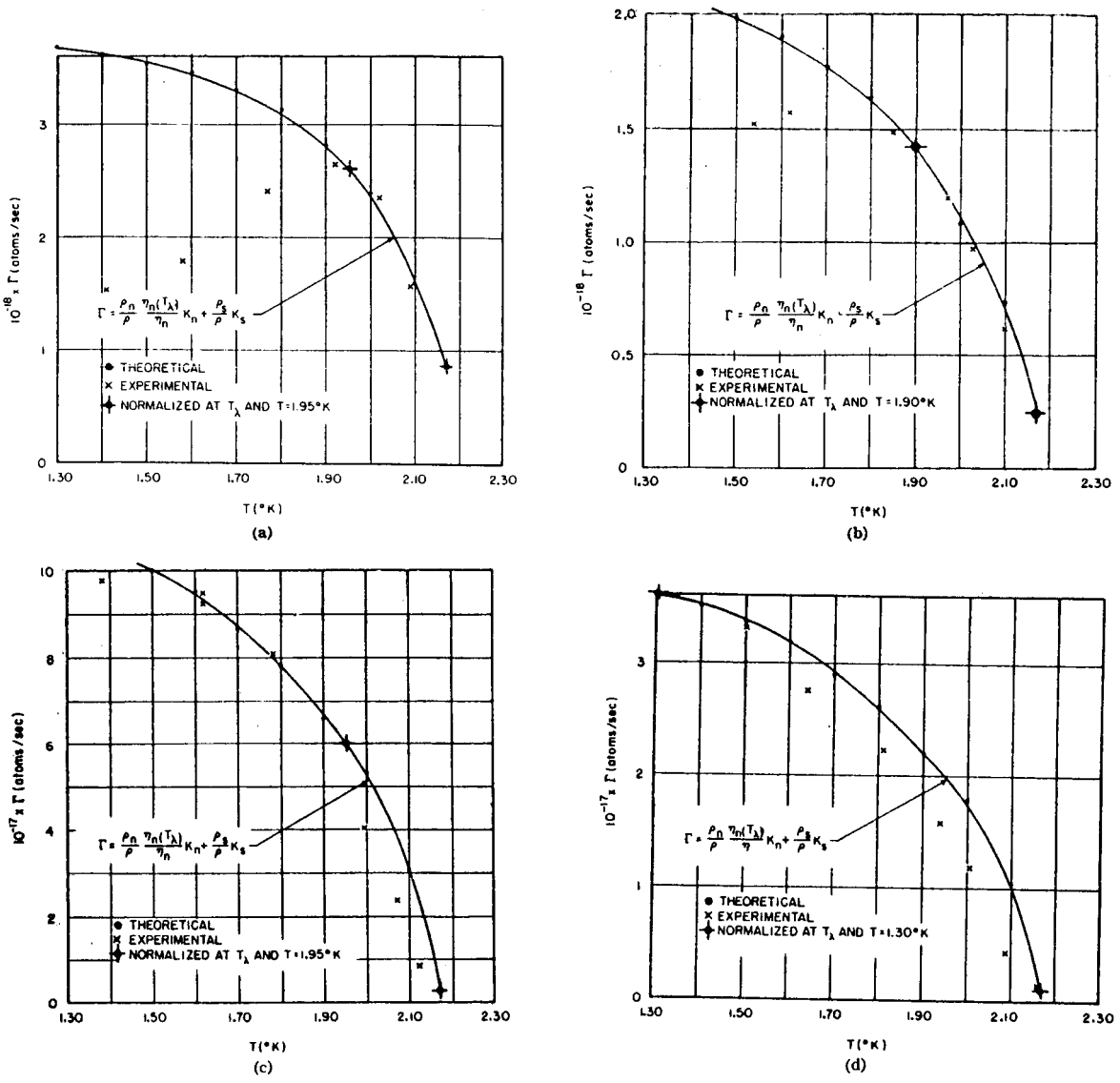

FIG. 10. Critical flow in channels of various sizes. (a) Size A channel at 3.0×10^6 V/cm; (b) Size B channel at 2.5×10^6 V/cm; (c) Size C channel at 2.0×10^6 V/cm; (d) Size D channel at 1.5×10^6 V/cm.

difference in the liquid between the entrance of the channel and the liquid-gas interface, and ΔT was the temperature difference between the bath fluid and the liquid-gas interface.

The thermomechanical pressure prevented the superfluid from penetrating the entire channel and flowing past the exit. The length of channel occupied by gas and the pressure drop in the gas were appropriate for the flow rate. The field induced flow was a second stronger indication that the penetration of the entire channel expected from the absence of superfluid viscosity and the net pressure acting on the liquid did not occur.

Inferences from the Occurrence of an Internal Interface

A flow increase proportional to the square of the electric field was deduced from the occurrence within the channel of the liquid-gas interface. The additional thermomechanical pressure, $\Delta P'$, necessary to counteract the electric pressure [cf. Fig. 2(g)] acting on the liquid resulted from the cooling of increased evaporation. From an assumption that the additional field-induced temperature difference $\Delta T'$ between the bath and the liquid-gas interface was given in analogy with (8) by

$$\rho S\Delta T' = \Delta P' \approx \Delta P_{12}^{(e)} \tag{9}$$

an additional proportional amount of heat flow to the liquid in the channel was associated with $\Delta P_{12}^{(e)}$. The rate of helium evaporation or the net mass flow was proportional to the heat flow to the liquid in the channel. Thus, $\Delta P_{12}^{(e)}$, which was proportional to E^2, caused the temperature difference between the liquid-gas interface

and the bath to increase by $\Delta T'$ with a proportional increase in mass flow.

Figures 2(f) and 2(g) show flow behavior at $T=1.4°K$, where only an 8% concentration of normal fluid was present to create liquid losses. When a voltage was applied electrostriction caused a sharp rise in pressure near the channel entrance. The pressure barely changed over most of the liquid region since no losses occurred in the superfluid flow and the amount of normal fluid present was small. Near the liquid-gas interface a sharp drop in pressure was closely compensated by a thermomechanical pressure gradient.

In recapitulation, from the observation that the liquid did not penetrate the entire channel it was argued that an electrostrictive pressure proportional to V^2 induced a commensurate augmentation of the flow rate. The deduction was in accord with the second observation that

$$\Gamma-\Gamma_0=f(T)V^2 \tag{10}$$

below the λ point. Further, at high values of electric field the flow remained constant, the superfluid then being driven at critical velocity.

In Figs. 10(a)–(d) some conjectured curves of Γ vs T at the highest values of applied field have been plotted which follow from these presumptions:

(a) The highest field drove the superfluid to critical velocity and the flow of superfluid was governed by

$$\Gamma_s=(L/M)(\rho_s/\rho)\rho A u_c=(\rho_s/\rho)K_s, \tag{11}$$

with the critical velocity assumed independent of temperature.

(b) The flow of normal fluid was proportional to the normal fluid density, inversely proportional to the viscosity η, and given by

$$\Gamma_n=(\rho_n/\rho)[\eta(T_\lambda)/\eta(T)]K_n, \tag{12}$$

with variable pressure drop and length of liquid in the channel neglected.

From (11) and (12) the theoretical curve became

$$\Gamma=\Gamma_n+\Gamma_s=(\rho_n/\rho)[\eta(T_\lambda)/\eta(T)]K_n+(\rho_s/\rho)K_s. \tag{13}$$

K_n and K_s were determined for a particular channel by normalizing from two points on the experimental curve. For channel sizes A and B a good fit was obtained between T_λ and 1.90°K where Γ began to decrease, i.e., where the liquid had reached the channel exit.

In channel size C the theoretical curve agreed with experiment in the temperature range 1.95 to 1.60°K. The applied field was smaller than for channel sizes A and B and was not driving superfluid to the critical velocity over the whole temperature range. In channel size D experimental points fell below the theoretical ones in the temperature range 1.30°K to T_λ. The applied field, which was smaller still, was insufficient to drive the superfluid to critical velocity (field was limited by dielectric breakdown).

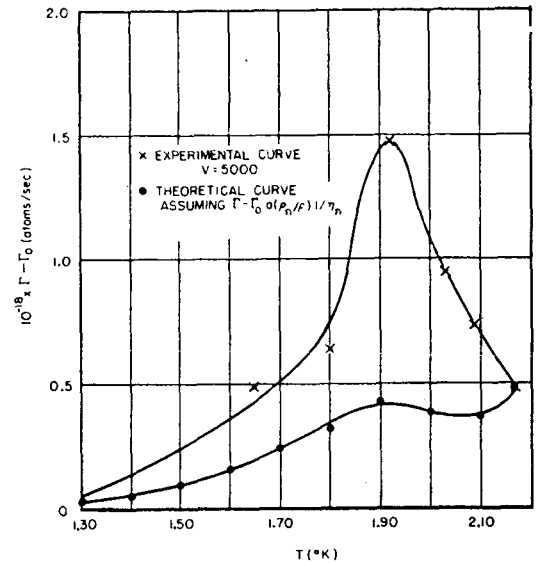

FIG. 11. Field-induced flow augmentation compared with conjectured normal fluid flow increase.

K_s, determined from the experimental data, made possible the calculation of the critical velocity. From experimental data for channel size A, K_s was found to be 3.8×10^{18} atoms/sec and u_c to equal 7 cm/sec with the channel thickness taken as 1.0×10^{-5} cm. Atkins[4] reported the critical velocity of superfluid helium in a powder packed channel to vary from 13 to 3 cm/sec as channel size varied from 10^{-5} to 4×10^{-4} cm.

That the electric pressures affected both the normal fluid and the superfluid may be seen in another way. If the field had affected only the normal fluid, $\Gamma-\Gamma_0$ would have been proportional to $(\rho_n/\rho\eta)V^2$. For a leak representative of channel size A Fig. 11 compares this function with flow increment at fixed voltage, with the value of $\Gamma-\Gamma_0$ at the λ point used as a reference. The surmised increase in flow of the normal fluid could not alone account for the actual one.

Displacement of the Transition Point

Experiments with an applied field of 1.5×10^6 V/cm ($V=4000$ V) to determine whether the λ point was shifted by electric field, are typified by the data of Fig. 12. A diffuse λ transition is indicated in the flow rates with and without field. From the data for various channel sizes, some showing the transition more sharply, it was concluded that a field of 1.5×10^6 V/cm shifted the λ point less than 0.02°K. Interpretation of the data was complicated by the interface temperature, which was several hundredths of a degree below the bath temperature and depended on the applied field strength.

Anomalous Flow Behavior

In a group of channels smaller than class D no flow was observed as the liquid-helium bath was initially

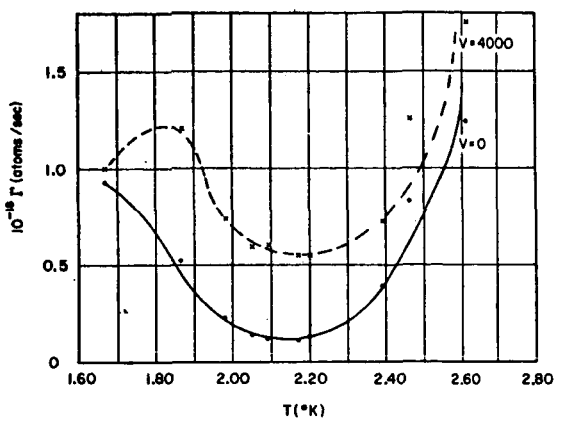

FIG. 12. Flow near the λ point in an *A* channel.

cooled from 4.2°K to a temperature below the λ point. After the sudden onset of flow at a temperature which ranged from 1.9 to 1.7°K, a normal pattern was observed throughout the entire temperature range. That is, flow occurred above the λ point and increased sharply below it.

Summary

In addition to the pressure gradients, gravitational forces, and thermomechanical forces ordinarily encountered in liquid-helium hydrodynamics, body forces of electrostrictive origin were present and dominant in this work. Superfluid flow at less than critical velocity was brought to flow at critical velocity, as long as part of the flow channel was filled with gas, by electric pressures which affected both the normal and superfluid components of the liquid. The apparatus may be considered to be an electrohydrodynamic flow regulator.

ACKNOWLEDGMENTS

Discussions of many aspects of the research with Professor H. W. Meissner, Professor F. Pollock, and Professor S. I. Rubinow were of substantial value. The authors wish to note, also, the assistance of W. Steinert in the construction of the apparatus.

MACROSCOPIC MODES OF He II

J. K. PERCUS
Courant Institute of Mathematical Sciences

Introduction

Excitations of many-body systems run the gamut from individual or one-particle motions to collective modes in which the particles all move in unison. It is the purpose of this note to show how knowledge of the low-lying individual levels of a many-boson system, i.e. He II, yields quite detailed information on the character of the high-lying macroscopically describable levels.

Free-particle States

An interactionless system will serve as prototype. The ground state for n particles in a unit periodic box is then simply $\psi_0 = 1$, and we may contemplate two complementary types of excitation,

$$\psi_1 = \Pi_i \chi(\mathbf{x}_i) \tag{1}$$

$$\psi_2 = \textstyle\sum_i \chi(\mathbf{x}_i) \tag{2}$$

(which are solutions of the n body problem if χ satisfies the one-body Schrodinger equation). Since the local velocity and mass density are given by

$$\mathbf{u}(\mathbf{x}) = \mathrm{Re}\langle \textstyle\sum \delta(\mathbf{x}-\mathbf{x}_i)\,\mathbf{p}_i\rangle/\rho(\mathbf{x}) \tag{3}$$

$$\rho(\mathbf{x}) = m\langle \textstyle\sum \delta(\mathbf{x}-\mathbf{x}_j)\rangle \tag{4}$$

it follows that in case (2), writing $\chi(\mathbf{x}) = n^{-1}\,\gamma + n^{-1/2}\,f(\mathbf{x})$ where $\int f(\mathbf{x})\,d\mathbf{x} = 0$, so that normalization requires

$$|\gamma|^2 + \int |f|^2\,d\mathbf{x} = 1,$$

$$\left.\begin{aligned} \rho_2(x)/mn &= |\gamma + n^{-1/2} f(\mathbf{x})|^2 + (1-1/n)\int |f|^2\,d\mathbf{x} \\ \rho_2(\mathbf{x})\,\mathbf{u}(\mathbf{x})/n &= \hbar\,\mathrm{Im}[(1-1/n)\int f^*\nabla f\,d\mathbf{x} + n^{-1/2}\gamma^*\nabla f(\mathbf{x}) + \\ &\quad + n^{-1} f^*(\mathbf{x})\nabla f(\mathbf{x})] \end{aligned}\right\} \tag{5}$$

The principal contributions arise from the $\mathbf{k} = 0$ ground state, emphasizing the one-body excitation character of ψ_2.

On the other hand, in case (1), all n bodies are correlated. If $\chi(\mathbf{x}) = \gamma + f(\mathbf{x})$, requiring once more $|\gamma|^2 + \int |f|^2\,d\mathbf{x} = 1$ for normalization, we find

$$\left.\begin{aligned} \rho_1(\mathbf{x})/nm &= |\chi(\mathbf{x})|^2 = |\gamma + f(\mathbf{x})|^2 \\ \mathbf{u}_1(\mathbf{x}) &= (\hbar/m)\,\mathrm{Im}\,[\nabla\chi(\mathbf{x})/\chi(\mathbf{x})] \\ \text{or}\quad \rho_1(\mathbf{x})\,\mathbf{u}_1(\mathbf{x})/n &= \hbar\,\mathrm{Im}\,[\gamma^*\nabla f(\mathbf{x}) + f^*(\mathbf{x})\,\nabla f(\mathbf{x})] \end{aligned}\right\} \tag{6}$$

the effect of the deviation from uniformity being markedly augmented.

Sound Waves

If the single particle momentum-energy relation is given by $\mathbf{p} = \hbar\mathbf{k}$, $\epsilon = \hbar\omega_{\mathbf{k}}[= \hbar^2 k^2/2m$ for consistency with (3)], propagation of a plane sound wave would correspond to

$$f(\mathbf{x}) = A\exp i(\mathbf{k}.\mathbf{x} - \omega_{\mathbf{k}}\,t)$$

At weak amplitude, the phonon excitation or second sound is then given by

$$\left.\begin{aligned} \rho_2(\mathbf{x})/mn &= 1 + 2n^{-1/2}\,A\cos(\mathbf{k}.\mathbf{x} - \omega_{\mathbf{k}}\,t) \\ \mathbf{u}_2(\mathbf{x}) &= (\hbar/m)n^{-1/2}\,A\cos(\mathbf{k}.\mathbf{x} - \omega_{\mathbf{k}}\,t) \end{aligned}\right\} \tag{7}$$

with group velocity $c_{\mathbf{k}} = \partial\omega_{\mathbf{k}}/\partial k$. The bulk compression or first sound now differs only by the replacement of $n^{-1/2}\,A$ by A. Thus at zero temperature, bulk properties of first and second sound are indistinguishable.

At temperature $T > 0$, the situation is altered. If we try to create a compression wave by the one-particle wave function replacement

$$\exp i(\mathbf{s}.\mathbf{x} - \omega_s t) \to \exp i(\mathbf{s}.\mathbf{x} - \omega_s t)\{1 + A\exp i[\mathbf{k}.\mathbf{x} - (\omega_{s+\mathbf{k}} - \omega_s)\,t]\} \tag{8}$$

then indeed the macroscopic occupation at $s = 0$ proceeds at zero temperature first or second sound velocity $c_{\mathbf{k}} = \partial\omega_{\mathbf{k}}/\partial k$. However, the remaining wave vectors have effective frequency $\omega_{s+\mathbf{k}} - \omega_s$. For a spectrum $\omega_{\mathbf{k}} = vk$, the peak of the thermal Bose distribution occurs at $s^* \sim 2\kappa T/\hbar v$. Since $k \ll s$ except for wavelengths of the order of atomic spacing or temperatures of microdegrees, then, as a qualitative assessment, the r.m.s. value of $\omega_{s+\mathbf{k}} - \omega_s$ immediately shifts from vk at $T = 0$ to $\sim vk/3^{1/2}$ for $T > 0$; the first sound velocity does likewise.

Hydrodynamic Modes

Let us examine the bulk motions given by (1). Assuming the one-body equation $-(\hbar^2/2m)\,\nabla^2\chi + U(\mathbf{x})\chi = i\hbar\dot{\chi}$, the fluid mass and momentum conservation laws

$$\left.\begin{aligned} \dot{\rho} + \nabla.(\rho\mathbf{u}) &= 0 \\ \dot{\mathbf{u}} + \mathbf{u}.\nabla\mathbf{u} + (1/m)\,\nabla[U - \rho^{-1/2}(\hbar^2/2m)\,\nabla^2\rho^{1/2}] &= 0 \end{aligned}\right\} \tag{9}$$

readily follow; $-\rho^{-1/2}(\hbar^2/2m)\,\nabla^2\rho^{1/2}$ is an effective quantum mechanical potential, tending to explode any localization of density. The flow pattern of (1) is characterized by the infinite singularities of $\mathbf{u}$, and these, according to (6), correspond to the nodes of χ. The basic non-singular flow is given by $\chi = \exp i\mathbf{k}.\mathbf{x}$, whence $\mathbf{u} = \hbar\mathbf{k}/m$, a 'moving state' of uniform velocity. An extension is the sound wave and volume counterflow previously considered.

If $\mathrm{Re}(\chi)$ and $\mathrm{Im}(\chi)$ vanish simultaneously at only a point, a point singularity in the flow appears; in the absence of symmetry, this is an exceptional case, as is that of a stationary point $\mathbf{u} = 0$. But $\mathrm{Re}(\chi)$ and $\mathrm{Im}(\chi)$ will usually vanish together on a line. The standard line singularity is a vortex, typefied by a local dependence $\chi = x + iy$, leading to

$$\mathbf{u} = (\hbar/m)(-y, x, 0)/(x^2+y^2) = (\hbar/m)\,\hat{\phi}/r$$

For example, a free particle wave function $\sin 2\pi x + i\sin 2\pi y$ in a periodic box produces a quartet of vortices; since $\rho \propto x^2 + y^2$, the fluid kinetic energy remains finite. Infinitely rapid oscillations can also yield a line singularity without vorticity, e.g.

$$\chi = \exp[i(x^2+y^2)^{-1}]$$

implies $\mathbf{u} \propto (x, y, 0)/(x^2+y^2)^2$, but these will not be of interest. Finally, surface singularities do not occur, but nulls do, either at real boundary surfaces or internal stagnation surfaces. In general, however, surface effects are best treated by a distortion engendered by a momentum-dependent generalization of χ.

Application to He II

The foregoing extends with surprising ease to interacting Bose systems which for the sake of simplicity will be taken in the ground state. If ψ_0 is the uniform ground state, we follow (1) and set

$$\psi = (\exp i \sum \lambda(\mathbf{x}_j))\,\psi_0 \tag{10}$$

where λ is a complex function of time as well as position. An immediate consequence of (3) is that $\mathbf{u}(\mathbf{x}) = \mathrm{Re}(\hbar/m)\,\nabla\lambda(\mathbf{x})$; the expression for $\rho(\mathbf{x})$ is less explicit. We now assume that low-lying modes are well represented by oscillations of the Fourier components of the matter density, $q_\mathbf{k} = \sum \exp i\mathbf{k}\cdot\mathbf{x}_j$ at frequencies $\omega_\mathbf{k}$, so that the ground state will satisfy

$$\dot{q}_\mathbf{k}\psi_0 = i\omega_\mathbf{k} q_\mathbf{k}\psi_0 \tag{11}$$

Further, in the absence of viscosity, shear modes propagate freely rather than oscillate, so that the transverse momenta annul ψ_0:

$$\sum \mathbf{k}\times\mathbf{p}_j \exp i\mathbf{k}\cdot\mathbf{x}_j\psi_0 = 0 \tag{12}$$

Equations (11) and (12) may be combined to read

$$\sum [\mathbf{p}_j f(\mathbf{x}_j) + f(\mathbf{x}_j)\mathbf{p}_j]\psi_0 = (\hbar/i)\sum G\nabla f(\mathbf{x}_j)\psi_0$$

where
$$Gf(\mathbf{x}) = \sum_{\mathbf{k}\neq 0} (2m\omega_\mathbf{k}/\hbar k^2) f_\mathbf{k} \exp i\mathbf{k}\cdot\mathbf{x} \tag{13}$$

for 'arbitrary' f. But now consider the Schrodinger equation with external field as well:

$$[\sum p_j^2/2m + V(\mathbf{x}_1 \ldots \mathbf{x}_n) + \sum U(\mathbf{x}_j)]\,\psi = i\hbar\dot{\psi}$$

for ψ of (10). By virtue of (13), this may be shown to be exactly satisfied if

$$\dot{\lambda}(\mathbf{x}) + (\hbar/m)\nabla\lambda(\mathbf{x})\cdot\nabla\lambda(\mathbf{x}) + (\hbar/2mi)G\nabla^2\lambda(\mathbf{x}) + U(\mathbf{x})/\hbar = 0 \tag{14}$$

our main result.

Discussion

To interpret eqn (14), let us write

$$\lambda = (m/\hbar)\phi - \tfrac{1}{2}i\ln\tilde{\rho} \tag{15}$$

for real ϕ and $\tilde{\rho}$. Taking imaginary and real parts of (14), and applying the gradient to the second of these and to (15), we have

$$\left.\begin{aligned} \partial\tilde{\rho}/\partial t + \mathbf{u}\cdot\nabla\tilde{\rho} + \tilde{\rho}G(\nabla\cdot\mathbf{u}) &= 0 \\ \partial\mathbf{u}/\partial t + \mathbf{u}\cdot\nabla\mathbf{u} - (\hbar^2/4m^2)\nabla[\tfrac{1}{2}(\nabla\ln\tilde{\rho})^2 + & \\ + G(\nabla^2\ln\tilde{\rho})] + \nabla U/m &= 0 \\ \mathbf{u} &= \nabla\phi \end{aligned}\right\} \tag{16}$$

which generalizes (9) [the relation between $\tilde{\rho}$ and ρ being tailored to convert the first of (16) to mass conservation].

The classification of hydrodynamic modes proceeds just as in the interactionless case, with the correspondence $\chi = \exp i\lambda$. A single-valued velocity potential ϕ necessarily produces a curl-free velocity field. However λ may be multi-valued in units of 2π, and hence ϕ by h/m. A singular line of multi-valuedness thus gives rise to a vortex whose strength must be quantized in units of h/m. The density field is then determined from (16) by the spectral operator G (with kernel $\sim 4mc/\hbar x^2$ for constant phonon velocity c) and recovers its uniform value within atomic dimensions.

Degeneration of steady flow into vortices is presumably the mechanism for damping superflow above critical velocity, and the velocities obtained kinematically for simple geometries from the above description are at least qualitatively correct. It may also be conjectured that the nature of the λ-point transition is due principally to an equilibrium of quasi-stationary quantized vortex modes; unlike those in the non-interacting case, they are not even in principle combinations of highly excited phonon modes, but rather constitute a qualitatively new branch of the spectrum.

This work is supported in part by the U.S. Atomic Energy Commission. The investigation was initiated by J. K. Percus in the Symposium on the Many-Body Problem. Interscience, (in press), and in N.A.S.A. Stevens Institute of Technology Cryogenics reports (unpublished).

The Use of Electric Fields in the Investigation of the Structure of Liquid and Solid Helium

ABSTRACT

Investigations are proposed involving an experimental and theoretical program designed to investigate various properties of the structure of helium both in its atomic form and in the aggregates of the liquid and solid states. The key to the possibilities of performing the experiments lies in the relatively weak electric fields existing in liquid and solid helium and the possibility of producing external fields almost comparable with the internal fields. It is proposed to examine a) the melting pressure curve for helium as a function of electric field b) the dielectric constant of helium as a function of pressure end electric field c) in the future, the effect of electric fields on the λ transition. From the results of these experiments one would expect to be able to gather at least corroborative evidence on a) the crystal structure of solid helium and evidence on b) the effect of Van der Waal interaction on the electric polarizability of helium c) the possibility of producing helium molecules d) the effective volume available to helium atoms in the liquid and possibly e) the effect of particle interactions on the Bose-Einstein condensation.

PROPOSED RESEARCH

1. General:

The program for which support is being requested has as its object the investigation of properties of liquid and solid helium which may shed light on their structure. The general approach will be to examine, with the use of large electric fields, the electrical properties of, the thermodynamics of, and the phase transition associated with helium. As a significant consequence will be information relevant to the understanding of the structure of atomic and (in the event of its existence) molecular helium.

II. Liquid-Solid Phase Transition

Much of the understanding that we have of the liquid-solid transition in helium is based on semi-qualitative arguments presented by London[1]. For the purposes of our discussion we will restrict ourselves to the temperature region in which the entropy change associated with the liquid solid phase transition vanishes. Although, at least in the preliminary stages of the experiment, the temperatures achieved will be above the values for which there is no entropy change, the assumption will serve as a fruitful model with which to work. Under this assumption the pressure required (about 25 atmospheres) to bring about the change to the solid phase is roughly given by

$$\Delta p = \frac{U_s - U_L}{V_L - V_s}$$

where U represents the internal energy and V the specific volume. The details of the arguments and the deviations resulting from quantum and kinetic effects will not be discussed except insofar as they relate to the experiment. The melting pressure is, in fact, given by the slope of the tangent line common to the internal energy curves of the solid and the liquid. In order, therefore, to make a prediction of the value of the melting pressure one requires the internal energy curves of the two phases. London and others[2] have made estimates of these functions based on rough but reasonable models for both the liquid and the solid. In doing this, estimates of the potential energy of the lattice and of the liquid were made and yielded results of the order of 50 or 60 cal/mol. Estimating from this, the average electric fields in the liquid or solid one gets fields of the order of

$$E = 3 \times 10^7 \text{ Volts/cm}$$

Thus, if fields between 10^6 and 10^7 Volts/cm can be achieved in helium, one can externally produce fields of the order of a reasonable large fraction of the internal fields.

One may now examine in a little detail the effect of the electric fields on the phase transition: A straightforward extension of the Clausius-Clapeyron Equation gives at constant temperature

$$\frac{\partial P}{\partial E} = \frac{\Delta \vec{P}}{\Delta V}$$

where $\frac{\partial P}{\partial E}$ is the derivative along the melting point curve, that is the rate of change of the melting pressure with external field. $\Delta \vec{P}$ is the change in the total polarization of a mole of helium and ΔV the change in a molar volume of helium in the phase transition. Introducing the Polarization Vector $P = \frac{\vec{P}}{V}$ and the electric susceptibility $= K-1$ one has

$$\frac{\partial P}{\partial E} = \frac{+\epsilon_0 E}{V_s - V_L}\left\{(K_s - 1)V_s - (K_L - 1)V_L\right\}$$

Now, in fact, the molar volume is a function of the electric field but this, although important for some aspects of the experiment, will be ignored for the present.

Then

$$\frac{\partial P}{\partial E} = +E\epsilon_0\left\{1 - \frac{K_s V_s - K_L V_L}{V_s - V_L}\right\}$$

which clearly vanishes for $K = 1$. However, K as can be seen from analyses of electrostrictive phenomena depends on V and one is left with two possibilities. Either K_s is the same function of the density as is K_L that is, presumably they both obey the usual Clausius-Mosotti equation or K_s is a different function of the density. Whether the first or second proposition is correct depends on the crystal structure of the solid[3]. For example, for any cubic structure the solid obeys the Clausius-Mosotti Equation as well as the liquid. For this case

$$\frac{\partial P}{\partial E} = +\epsilon_0 E\left\{1 - \frac{K_L(V_s)V_s - K_L(V_L)V_L}{V_s - V_L}\right\}$$

$$\cong +\epsilon_0 E\left\{1 - K_L(V_L) - V_s\left.\frac{\partial K_L}{\partial V}\right|_{V_L}\right\}$$

where higher order terms in ΔV have been neglected

$$\frac{\partial P}{\partial E} \cong +\epsilon_0 E\left\{1 - K_L - \frac{V_s}{V_L}\left(V\left.\frac{\partial K}{\partial V}\right)\right|_{V_L}\right\}$$

which for the Clausius-Mosotti Equation

$$\frac{\partial P}{\partial E} \cong +\epsilon_0 E \left\{ 1 - K_L + \frac{V_S}{V_L} \frac{(K_L-1)(K_L+2)}{3} \right\}$$

giving

$$\Delta p = -\frac{\epsilon_0 E^2}{2} (K_L-1) \left\{ 1 - \frac{V_S}{V_L} \frac{(K_L+2)}{3} \right\}$$

and if

$$\frac{V_S}{V_L} \sim .9 \qquad \Delta p \sim -\frac{.1\,(K_L-1)\epsilon_0 E^2}{2}$$

for $K_L = 1.06$ and for fields of the order of 3×10^6 v/cm, $\Delta p \sim 20$ mm of mercury.

Thus one expects an easily measurable change in the melting pressure of helium produced by the external field. There is still the other possibility namely that K_S is not given by the Clausius-Mosotti Equation because the crystalline structure does not possess the proper symmetry. This should then be reflected in a different pressure change presumably distinguishable from that occurring in the other case. There is then here immediate applicability to the question concerning the nature of the newly found phase of solid helium[4]. It should be either possible to make at least limiting statements about the structure of the crystals or assuming the structures, some statement about the constancy of the atomic polarizability of the helium.

All of the preceding has dealt with the gross effect of changing the internal energy of the helium. Of further interest is the possibility of examining the shape of the internal energy curve by examining the effect of a small known change in the internal energy. Roughly speaking in the region of the internal energy minima corresponding to the liquid and solid phases,

the internal energy curve may be represented by a parabola. One can write in the absence of an external field

$$U_L = A_L + B_L (V - V_L)^2$$

$$U_S = A_S + B_S (V - V_S)^2$$

and the values of the A's and the B's will be determined by the sizes of the potential energy and zero point energy. By adding to the U's, a known increment, and examining the change in the slope of the common tangent that is, the change in the pressure, some idea of the values of the coefficients can be achieved.

The experiment to examine this effect is already being prepared. The blocked capillary method[5] will be used to determine the melting pressure curve. The experiment as designed at present will allow a direct comparison of the field free melting pressure with that in the presence of the electric field. Since the absolute pressure is of much less significance than the change, this technique will allow us to measure the important effect with a relatively high degree of accuracy. While the percentage change in the pressure will probably be only of the order of .1% the value of the change directly measured should still be of the order of 20 mm of mercury. Assuming that, if necessary, an oil manometer can be used, readings of accuracy of 1 part in 250 should readily be made. The inaccuracies in the field measurements will be a more serious problem but it is expected that at least the gross effect (that ignoring the shape of the internal energy curve) should be measurable. While in the initial capillaries examined ellipticities in the bore shape have been observed, the problem of determining the fields in the occurring geometry theoretically is not formidable.

Studies are under way to determine the consistency of bore size which presumably will be the limiting factor. The electric field will be provided by a fine wire threaded through the capillary and preliminary studies show that the wire size will not vary sufficiently to cause serious variations in the electric field.

There have been reported results[6] in which fields of 10^6 V/cm have been achieved before breakdown in helium. If this figure turns out in fact to be limiting the effects will be smaller but they will still be measurable presumably to an accuracy of a few percent. It should be added, however, that unpublished results by workers at Stevens seem to indicate that at least in narrow channels, considerably higher fields are attainable[7].

It is forseen that in the future more accurate determinations of the pressure change may be essential for examining some of the effects thus far mentioned. Plans are already under consideration, should this indeed become necessary.

III. Dielectric Measurements

As a counterpart to the phase change investigation there is a program planned for investigating the thermodynamics and electrostatics of liquid helium. There are a number of questions whose answers would be of considerable interest which may be illuminated by the proposed experiments. It is well known that non-polar liquids presumably have dielectric constants which vary with density in accordance with the Clausius-Mosotti Equation[3]. The assumptions that are made in the derivation are:

1) Randomness of angular distribution of atoms
2) Non polarity of molecules
3) Field independence of the particle polarizability
4) Independence of polarizability of particle interaction.

For helium assumptions 1) and 2) are almost certainly valid. The validity of 3) and 4) is doubtful and depends on detailed understanding of the electron configuration in the helium. It is for example, not fully understood how the Van der Waal interaction effects the atomic polarizability of helium. Thus, since the interaction between atoms is space dependent a change in density might effect the atomic polarizability. Thus in the expression for the Clausius-Mosotti Equation

$$\frac{K-1}{K+2} = \frac{4\pi\rho}{3M}\alpha$$

α is the atomic polarizability which, in principle, will depend on both the density and the electric field.

In the extreme, conceivable case in which the helium atoms form either molecules or clusters the effect on the polarizability may be measurable. The experiment planned is the measurement of the dielectric constant of liquid helium as a function both of pressure and electric field. The effects that may be studied may be readily enumerated.

1) The Clausius-Mosotti Equation may be verified. By plotting for small fields $\frac{K-1}{K+2}$ vs the density an estimate of the constancy of the polarizability with changing Van der Waal interaction can be made.

It should be noted that the atomic electric polarizability of helium has been measured over a wide range of densities - it has been substantially constant over this range. This should not be extrapolated to even greater densities as it is in the region approaching close packing where differences might occur.

2) An increase in the pressure or density results in a decrease in the available volume to an atom of helium and therefore an increase in the probability of finding a bound helium molecule if it exists.

3) Measuring the polarizability of the helium atom as a function of electric field by dielectric constant measurement will allow a check on atomic calculations on helium. Furthermore, the increase in electric field increases the interaction between atoms and for a given density should appear as an increased Van der Waal interaction.

4) The question of the existence of a bound state for the helium molecule is still an open one[8]. Various interaction potentials give differing predictions as to the existence or non-existence of the bound state. At any rate, there is either none or one state whose binding energy is very close to zero (10^{-6} e.v.). In liquid helium, however, the existence or nonexistence of the bound state can, one would expect, produce very profound effects regardless of the small value of the binding energy. For if an atom in the liquid can be considered to be confined in a volume of the order of the volume per atom, the number of states available to the atoms of the dissociated molecules will be small. Thus the difference between the existence and non-existence of a bound state may be quite sharp in its effect on the liquid. Now in view of the fact that the difference between potentials predicting the existence of a bound state and those predicting the lack of existence of the state is very small, it is quite conceivable that an increased dipole-dipole interaction due to an applied electric field might allow for a bound state that in the absence of an external field would not exist. In view of the preceding arguments a newly appearing bound state might then have effects on the dielectric constant as well as other properties of the liquid helium. Eventually, an attempt should be made to find an isotropy in the fluid in a plane containing the direction of the electric field.

The experiments to measure the effect on the dielectric constant will be performed in two ways. One is an extension of the method to be used in the liquid-solid transition measurement in which the electrostrictive pressure is measured as a function of pressure (density) and field strength. The other more accurate method will be to measure the capacitance of a helium filled capacitor using a sensitive frequency measuring device.

In conjunction with this experimental work there is room and considerable need for theoretical calculations on atomic helium. The theoretical predictions required are:

1) The effect of a change in density on the probability of molecular helium dissociation.
2) The effect of the Van der Waal forces on helium polarizability.
3) The effect of molecular structure on polarizability.
4) The effect of the increased interaction due to fields on the the existence or non-existence of bound states of the helium molecule.
5) The probability of the formation of large clusters or chains of helium atoms[9].

IV. The Superfluid Phase Transition

There has been at Stevens work on the effect of electric fields on helium flow near and below the lambda temperature. While this work continues, another experiment is being planned here involving the measurement of heat conduction near the transition temperature. Presumably the position and value of the point depends on the interaction between the particles. As an argument to make this plausible one can point out that

lacking any interaction between particles a predicted phase transition (the Bose-Einstein condensation) would take place at a temperature above 3° rather than the observed 2.2°. Thus, if by imposing an electric field, the effective interaction between the atoms can be altered, one might expect a change in the λ point temperature.

Plans are at present to examine this by investigating heat induction through channels of varying size. Two chambers may be connected by a capillary containing a fine wire to produce the field. To the smaller of the two heat can be supplied at a temperature just below the λ point at such a rate that the conduction through the helium in the capillary just equals the input. Then, if the electric field is applied, a shift in the λ point should reflect itself in a change in the conduction and a resulting temperature change.

V. Hydrodynamic Aspects

In the less immediate future are planned experiments which deal with the flow of superfluid helium. Stated briefly they include motion of small material objects through superfluid helium, low speed rotation of liquid helium and scattering of sound by inhomogeneities in liquid helium (such as He^3 atoms).

Bibliography:

1) See London "Superfluids Vol. II"

2) Pekeris, C. L. Phys. Rev. 79, 884 c (1950)

3) See Frölich "Theory of Dielectrics"

4) Vignos and Fairbank Phys. Rev. Lett. 6, 6 P 265 (1961)

5) Swenson Phys. Rev. 89, 538 (1953)

6) Edwards and Blank Bull. Am. Phys. Soc. 5, 1 (1961)

7) J. Fajans, private communication

8) See Hirschfelder "Molecular Theory of Liquids and Gases"

9) Atkins Phys. Rev. 116, 1339 (1959)